Broadband Fourier-Domain Mode-Locked Lasers

Kevin HSU[1], Panomsak MEEMON[2,3], Kye-Sung LEE[3], Peter J. DELFYETT[2], and
Jannick P. ROLLAND[3,2]

[1]*Micron Optics, Inc., Atlanta, Georgia 30345, USA*

[2]*CREOL, The College of Optics and Photonics, University of Central Florida, Orlando, Florida 32816, USA*

[3]*The Institute of Optics, University of Rochester, Rochester, New York 14627, USA*

*Corresponding author: Kevin HSU   E-mail: khsu@micronoptics.com

Abstract: Broadband, high-speed wavelength-swept lasers can substantially enhance applications in optical coherence tomography, chemical spectroscopy, and fiber-optic sensing. We report the demonstration of Fourier-domain mode-lock lasers operating at about 90 kHz effective sweep rate over a 158 nm sweep range using a single-band design and over a 284 nm sweep range across the 1.3 μm to 1.5 μm wavelength spectrum using a unique broadband design. A novel dual-detection full-range Fourier-domain optical coherence tomography system is developed which provides 7 μm axial resolution (in air) at about 90 kHz axial scan rate for mirror-image resolved Doppler imaging in a human finger and an African frog tadpole.

Keywords: Fourier-domain mode-locked laser, swept laser, tunable laser

1. Introduction

High-speed wavelength-swept laser technology offers versatile applications in optical frequency domain imaging (OFDI) [1–3], bio-chemical spectroscopy [4], and fiber-optic sensing [5]. Particularly in recent years, swept laser technology has been critical in advancing OFDI applications in the field of biomedical imaging (i.e., optical coherence tomography) [6–8] and industrial imaging, imparting the advantages of real-time *in vivo* diagnostics and high sensitivity. This technology's broader reach can be seen in its applications in dynamic absorption spectroscopy and chromatic confocal microscopy. Two general classes of swept laser have been driving the advance in the aforementioned applications:

One is continuous-wave (CW) swept laser system [1, 2] and the other is Fourier domain mode-locked (FDML) laser system demonstrated recently by Huber *et al.* [6].

The typical configuration of a CW swept laser incorporates a semiconductor optical amplifier (SOA), a high-performance fiber Fabry-Perot tunable filter (FFP-TF), and the associated isolators and couplers to form a unidirectional fiber ring laser (Fig. 1 (without fiber coil)). This general design embodies the collective advantages of SOA broad gain-bandwidth with direct modulation capability, FFP-TF wide tuning ranges (i.e., free spectral range (FSR) > 200 nm), high finesse (1,000 to 20,000), low loss (< 2 dB), and fast scan rates. This class of swept laser system operates at arbitrary sweep rates, thus bears no relation to laser cavity resonance frequency and exhibits the following unique features: 1) Speed limitation: In cavity-tuning the maximum tuning speed is usually limited by the time-constant of the laser to build up lasing from the amplified

stimulated emission (ASE) background. This depends on filter function, ASE intensity, saturation power, laser gain, and cavity roundtrip time [2]. Initially the output power decreases gradually with the increasing scan rates. As the scan speed increases beyond the point for the amplifier to reach saturation, the output spectrum will begin to degrade rapidly. Ultimately, at excessive high scan frequencies, the light on average makes only one pass from SOA to filter and the cavity operates like a scanned incoherent source. Because lasing is built up repeatedly from ASE as the filter is tuned in wavelength, the filter bandwidth and cavity length must be optimized for specific high-speed applications. 2) Dynamic linewidth: Contrary to static linewidth, which depends strongly on the homogeneity of the gain medium, the dynamic linewidth is affected by the sweeping speed and constrained by filter bandwidth. 3) Spectral asymmetry: There is a strong spectral asymmetry between forward scans (from short to long wavelengths) and backward scans (from long to short wavelengths). This is caused by frequency downshift through intraband four-wave mixing within the SOA [9]. Scanning the filter in the same direction (forward scan) as the frequency shift allows intracavity light to experience less loss and enables higher lasing power and higher tuning speed operation. In general, a practical sweeping rate limit for CW swept lasers is in the range of about 20 kHz.

To overcome the speed limitations imposed by CW swept laser designs, a revolutionary FDML technique was demonstrated in 1310 nm and 1060 nm spectral regions [6, 7]. As illustrated in Fig. 1, this laser configuration is similar to standard ring-cavity design, except that FFP-TF is tuned in harmonic resonance to the fundamental cavity resonance that has been reduced by adding an additional length of fiber delay loop to match suitable electro-mechanical scan rates of FFP-TF. Rather than relying on repetitive transient built-up from ASE while the filter is tuned in wavelength, the SOA is seeded by the light from the previous frequency sweep with respect to individual frequency sweep components.
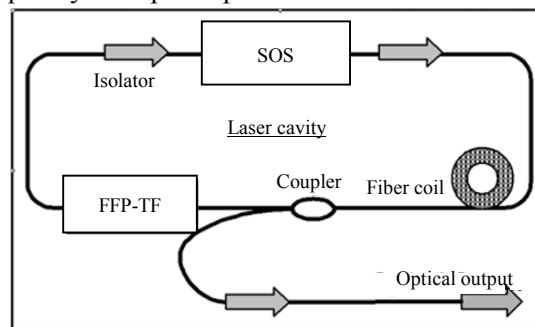

Fig. 1 Schematic of a single-band FDML laser module. The ring-cavity consists of a SOA as the gain medium, a FFP-TF for wavelength tuning, a fiber coil to set the cavity resonance frequency, isolators to enforce unidirectional lasing, and a fiber coupler for output coupling.

The FDML swept lasers have the advantage of high-speed, narrow linewidth, and high phase stability, and extensive effort has been invested in increasing sweep bandwidth and speed. In regard to sweep bandwidth, current FDML lasers using a single SOA have limited full-width-half-maximum (FWHM) sweep range of less than 117 nm for OFDI applications [8]. One approach to broaden the sweep range by combining two SOAs in parallel was first demonstrated in 1.3 μm wavelength band in CW swept laser mode using a polygon scanner at 20 kHz sweep frequency [10], which yielded a FWHM of 132 nm over 145 nm full range. Later a similar attempt in a FDML laser was demonstrated to provide slightly wider FWHM of 136.5 nm over 160 nm full range at much higher sweep frequency of 91.2 kHz (bilateral) [11]. However, because two SOAs have substantially overlapped in gain spectra, this design requires using two 3-dB couplers to combine two SOAs, adding significant cavity loss which compromises lasing range and output power.

In this work, we first demonstrate that a FDML laser of FWHM of 158 nm can be achieved by using a single-band design. Next, by using a broadband design, the feasibility of a 284 nm sweep range across 1.3 μm to 1.5 μm dual wavelength spectra is demonstrated.

2. Single-band FDML

By using a combination of high performance components to form single-band FDML laser as illustrated in Fig. 1, we have been able to obtain a FWHM sweep range as wide as about 158 nm (from 1252 nm to 1410 nm) at an effective sweep rate (bilateral) of 89.2 kHz as shown in Fig. 2. Note that due to the sinusoidal drive waveform, the temporal sweep profile is distorted accordingly, with most of the spectral range compressed in the middle of the sweep profile. In this arrangement, the FFP-TF has a FSR of about 160 nm, a bandwidth of about 0.2 nm, and a loss of less than 2 dB. The current FFP-TF design has a first-order electro-mechanical resonance near 45 kHz to 50 kHz. Therefore the total fiber cavity length (including fiber delay loop (Corning SMA28-e)) was designed for length of 4500 m. The SOA has a peak gain of 32.9 dB at 1304 nm, a bandwidth of about 46 nm, and a 3-dB saturation power Psat-3dB of 12.4 dBm. The output-coupling ratio of fused coupler is 20%, which provides an average output power of 5.6 mW.
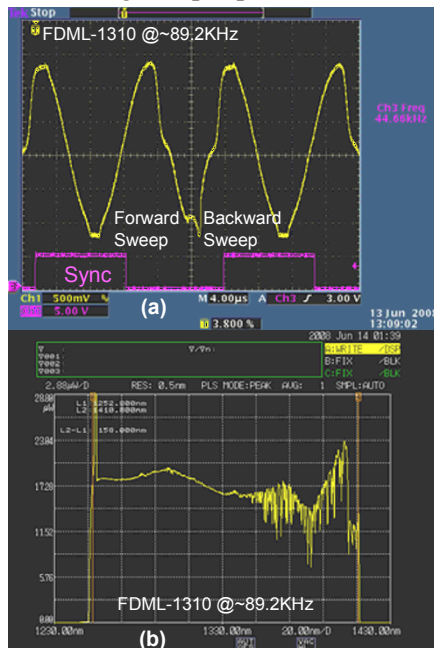

Fig. 2 Single-band 1310 nm FDML laser performance: (a) temporal swept laser profile at 89.2 kHz double-sided sweep rate and (b) swept optical spectrum showing a FWHM sweep range of 158 nm (from 1252.0 nm to 1410.0 nm).

3. Broadband FDML

To achieve broadband FDML, we chose to concatenate the adjacent spectral regions (1.3 μm and 1.5 μm) in a parallel configuration as illustrated in Fig. 3. The design consists of SOAs and isolators of adjacent bands arranged in a parallel-configuration, which is in turn coupled through two wavelength division multiplexers (WDMs) to complete the broadband ring-cavity. Two main technical challenges here are the ultra broadband component design and the requirements for bridging the dual spectra. The critical broadband components include a unique FFP-TF that provides FSR of 336.6 nm, bandwidth of 0.2 nm, loss of 1.5 dB, and a fiber coupler for 20% output coupling. A fiber delay loop of 4500 m is included to set the cavity resonance frequency to 45 kHz. In addition to the challenges of maximizing the sweep range, the overlap region must be optimized to minimize discontinuity and the interference arising from equivalent Mach-Zehnder interferometric configuration of parallel SOA paths. In this regard, the SOA gain spectra and the WDM crossover region must be well matched. In our current work, two SOAs have the following parameters: $SOA_{1.3}$: peak ~ 1299 nm, gain ~ 32.6 dB, bandwidth ~ 46.2 nm, and Psat-3dB ~ 12.4 dBm; $SOA_{1.5}$: peak ~ 1421 nm, gain ~ 21.8 dB, bandwidth ~ 61.7 nm, and Psat-3dB ~ 13 dBm.
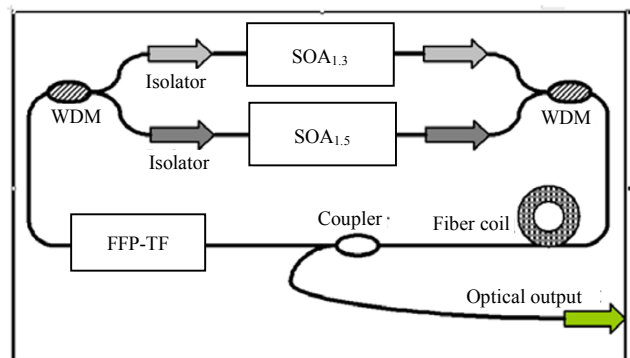

Fig. 3 Schematic of a broadband FDML module (the design consists of SOAs and isolators of adjacent bands arranged in a parallel configuration, then coupled through two WDMs to complete the ring-cavity, and the broadband components include a FFP-TF for wavelength tuning, a fiber coil to set the cavity resonance frequency, and a fiber coupler for output coupling).

Tested separately in single-band CW swept laser mode, 1.3 μm and 1.5 μm SOAs can respectively provide lasing from 1240 nm to 1403 nm and from 1374 nm to 1538 nm, indicating a substantial overlap region around 1400 nm. The custom-fabricated WDM has a cross-over point centered at 1400 nm and an isolation level of 2 dB – 3 dB, as illustrated in Fig. 4. This low isolation is important to minimize the spectral gap bridging two adjacent bands.
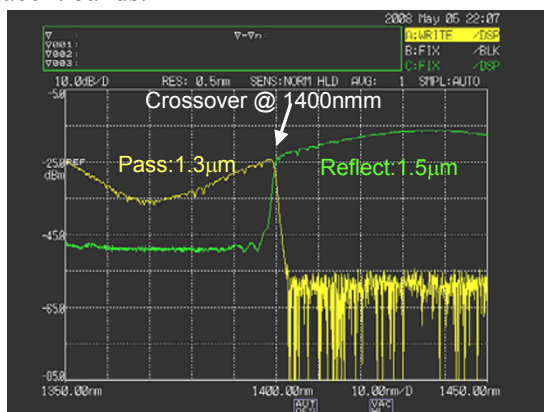

Fig. 4 Spectral characteristics of the WDM, having a band cross-over point centered at 1400 nm and an extinction of 2 dB.

An initial test of parallel configuration in CW sweep mode at 100 Hz drive frequency without fiber delay loop shows a sweep range from 1251 nm to 1534 nm, an average power P_a of 6.48 mW, and a discontinuity of about 5 dB as shown in Fig. 5. Under broadband FDML operation driven at 44.5 kHz sinusoidal frequency, an ultra broadband spectrum at about 89 kHz bilateral sweep frequency is generated over a sweep range from 1252.8 nm to 1396.8 nm and from 1400 nm to 1536.8 nm, with an average output power of 3.5 mW. As demonstrated in Fig. 6, in spite of 4 nm spectral gap and 20-dB discontinuity, high-speed FDML operation can be obtained over a total range of about 284 nm and fiber dispersion over such a large range is not a limiting factor. The additional loss in fiber delay loop is one significant cause of the crossover gap and we expect that this can be improved by fusion splicing to all fiber connectors.
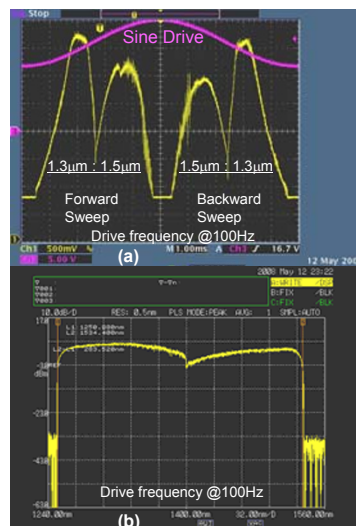

Fig. 5 Broadband CW swept laser performance at 100 Hz drive frequency, without fiber delay loop: (a) temporal swept laser profile and (b) swept optical spectrum showing a sweep range of about 283 nm and a discontinuity of about 5 dB.
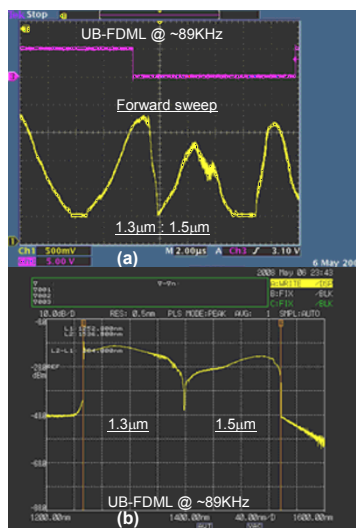

Fig. 6 Ultra broadband FDML laser performance at 89 kHz sweep frequency: (a) temporal swept laser profile and (b) swept optical spectrum showing a sweep range of about 284 nm, a wavelength gap of about 4 nm, and a discontinuity of about 20 dB.

4. Imaging application

We designed and developed a novel full-range Fourier domain optical coherence tomography (FD-OCT) system referring to dual-detection full-range FD-OCT (DD-FDOCT) that enables instantaneous retrieval of quadrature components of complex interferometric signal [12]. The DD-FDOCT system enables full range imaging without

loss of speed. Importantly, it is less sensitive to phase error generated by involuntary movements of subject in comparison to other established full range OCT systems because it uses two signals with a phase difference of $\pi/2$ obtained simultaneously from two detecting arms to remove mirror images at all depths. This developed FD-OCT system benefits from the broad bandwidth (158 nm) of single-band FDML laser so that it enables 7 μm axial resolution in air (wider than theoretical value due mainly to non-Gaussian spectrum), which is the highest axial resolution achieved among swept source based OCT at 1300 nm using a single SOA. The DD-FDOCT was applied to an *in vivo* human finger. We achieved a full range OCT image shown in Fig. 7 that consisted of 500 axial (A)-scans and 500 points per A-scan. In Fig. 7(a) the image using only a single detector shows the folded artifact image, while the artifact-free image generated in DD-FDOCT system is shown in Fig. 7(b). Both images are 2 mm by 2 mm in cross section.
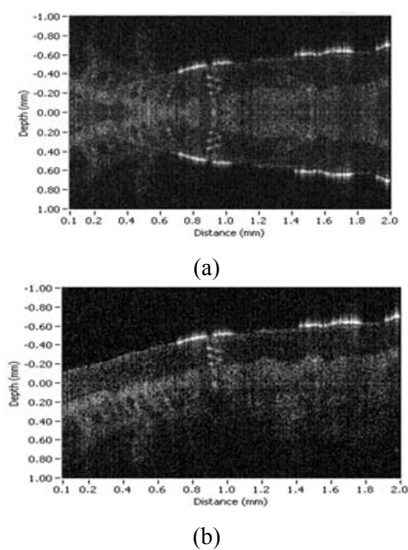

(a)

(b)

Fig. 7 Biological imaging (*in vivo* human finger): (a) real image and mirror image overlapped OCT image using a conventional FD OCT system and (b) mirror image removed OCT image using the DD-FDOCT system.

Moreover, the application of FDML laser for phase-resolved Doppler OCT was presented [13, 14]. The system exhibited high Doppler phase stability and allowed for flow monitoring over wide range of

detectable flow velocity. The capability of DD-FD-OCT for phase-resolved Doppler imaging was investigated [13]. One of the advantages of DD-FD-OCT to Doppler imaging is that the full-range signal is achieved without manipulation of phase relation between consecutive axial lines. Therefore, the phase information of full-range signal acquired by DD-FD-OCT is almost identical to that acquired by conventional FD-OCT. Hence, it can be used for Doppler detection. Figure 8 shows Doppler imaging of an African frog tadpole by using full-range DD-FD-OCT system. Intensity images of the tadpole captured at a location close to heart chamber are shown in Figs. 8(a) and 8(b) for conventional FD-OCT and full-range DD-FD-OCT, respectively, processed from the same set of acquired spectra. Furthermore, Figs. 8(c) and 8(e) are zoom-in versions of the intensity images at the region indicated by the white dash box in Fig. 8(b) that contains one of the main blood vessels connected to heart chamber. The flow activity can be observed from Doppler images (Figs. 8(d) and 8(f)) where the mirror Doppler is completely suppressed in full-range mode (Fig. 8(f)) as compared with that process in conventional mode (Fig. 8(d)).
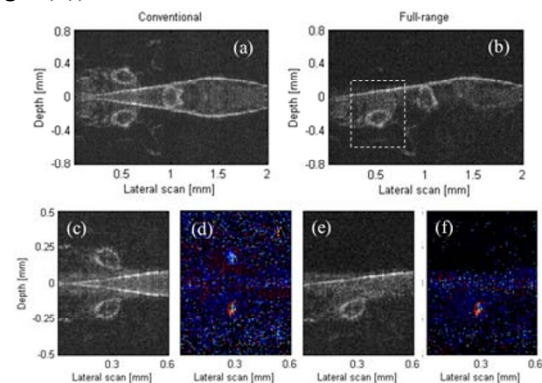

Fig. 8 Doppler images of an African frog tadpole: (a) and (b) are intensity images taken by conventional FD-OCT and DD-FD-OCT, respectively, (c) and (e) are zoom-in of (a) and (b) within the area marked by white dash box in (b), (d) and (f) are Doppler images corresponding with structural images in (c) and (e), respectively.

5. Conclusions

We have demonstrated a FDML swept laser exhibiting a wide FWHM sweep range of about 158 nm at 89.2 kHz sweep frequency in 1.3 μm band by using a single SOA in an optimized low-loss ring cavity. To achieve broadband FDML operation, we designed a parallel SOA configuration to accommodate adjacent spectral windows and incorporate broadband optical components in common path. Indeed, a broadband spectrum at about 89 kHz sweep frequency was generated over a sweep range from 1252.8 nm to 1396.8 nm and from 1400 nm to 1536.8 nm, with an average output power of 3.5 mW. We expect that 4 nm gap near 1400 nm wavelength region can be bridged by reducing cavity loss and by a custom fabricated 1.5 μm SOA with a blue-shifted spectrum to boost the gain over WDM crossover region. Such high-speed broadband FDML lasers can significantly enhance the applications in high-resolution imaging and dynamic spectroscopy.

In the application of FDML lasers to high-speed and high-resolution *in vivo* biomedical imaging, a novel dual-detection full-range Fourier domain optical coherence tomography system is developed which provides 7 μm axial resolution (in air) at about 90 kHz A-scan rate for mirror-image resolved Doppler imaging in a human finger and an African frog tadpole.

Acknowledgement

References

[1] M. A. Choma, K. Hsu, and J. A. Izat, "Swept source optical coherence tomography using an all-fiber 1300nm fiber ring swept laser source," *J. Bio-Medical Optics*, vol. 10, no. 4, pp. 044009(1−6), 2005.

[2] R. Huber, M. Wojtkowski, K. Taira, J. G. Fujimoto, and K. Hsu, "Amplified, frequency swept lasers for frequency domain reflectometry and OCT imaging: Design and Scaling Principles," *Optics Express*, vol. 13, no. 9, pp. 3513−3528, 2005.

[3] J. Zhang, Q. Wang, B. Rao, Z. Chen, and K. Hsu, "Swept laser source at 1 micron for Fourier domain optical coherence tomography," *Appl. Physics Lett.*, vol. 89, no. 7, pp. 073901(1−3), 2006.

[4] L. A. Kranendonk, X. An, A. W. Caswell, R. E. Herold, S. T. Sanders, R. Huber, J. G. Fujimoto, Y. Okura, and Y. Urata, "High speed engine gas thermometry by Fourier-domain mode-locked laser absorption spectroscopy," *Optics Express*, vol. 15, no. 23, pp. 15115−15128, 2007.

[5] K. Hsu, T. Haber, J. Mock, J. Volcy, and T. W. Graver, "High-speed swept-laser interrogation system for vibration monitoring," *Structural Health Monitoring*, Lancaster, PA: DEStech Publications, 2003, pp. 1043−1050.

[6] R. Huber, M. Wojtkowski, and J. G. Fujimoto, "Fourier Domain Mode Locking (FDML): A new laser operating regime and applications for optical coherence tomography," *Optics Express*, vol. 14, no. 8, pp. 3225−3237, 2006.

[7] R. Huber, D. C. Adler, V. J. Srinivasan, and J. G. Fujimoto, "Fourier domain mode locking at 1050 nm for ultra-high-speed optical coherence tomography of the human retina at 236,000 axial scans per second," *Optics Letters,* vol. 32, no. 14, pp. 2049−2051, 2007.

[8] D. C. Adler, S. W. Huang, R. Huber, and J. G. Fujimoto, "Photothermal detection of gold nanoparticles using phase-sensitive optical coherence tomography," *Optics Express*, vol. 16, no. 7, pp. 4376−4393, 2008.

[9] A. Bilenca, S. H. Yun, G. J. Tearney, and B. E. Bouma, "Numerical study of wavelength-swept semiconductor ring lasers: the role of refractive index nonlinearities in semiconductor optical amplifiers and implications for biomedical imaging applications," *Optics Letters,* vol. 31, no. 6, pp. 760−762, 2006.

[10] W. Y. Oh, S. H. Yun, G. J. Tearney, and B. E. Bouma, "Wide tuning range wavelength-swept laser with two semiconductor optical amplifiers," *IEEE Photon. Technol. Lett.*, vol. 17, no. 3, pp. 678−680, 2005.

[11] M. Y. Jeon, J. Zhang, Q. Wang, and Z. Chen, "High-speed and wide bandwidth Fourier domain mode-locked wavelength swept laser with multiple SOAs," *Optics Express*, vol. 16, no. 4, pp. 2547−2554, 2008.

[12] K. Lee, P. Meemon, W. Dallas, K. Hsu, and J. P. Rolland, "Dual detection full range frequency domain optical coherence tomography," *Opt. Lett.*, vol. 35, no. 7, pp. 1058−1060, 2010.

[13] P. Meemon, K. S. Lee, and J. P. Rolland, "Doppler imaging with dual-detection full-range frequency domain optical coherence tomography," *Biomed. Opt. Express,* vol. 1, no. 2, pp. 537−552, 2010.

[14] P. Meemon and J. P. Rolland, "Swept-source based, single-shot, multi-detectable velocity range Doppler optical coherence tomography," *Biomed. Opt. Express*, vol. 1, no. 3, pp. 955−966, 2010.